Transactions of JASCOME Vol. 7, No. 2 (March, 2008), Paper No. 06-080317 JASCOME

EFFECTS OF STRAIN RATE AND RELAXATION RATE ON ELASTIC MODULUS OF SEMI-CRYSTALLINE POLYMER

Hiroyuki MAE[1)], Masaki OMIYA[2)] and Kikuo KISHIMOTO[3)]

1) Honda R&D Co., Ltd. (4630 Shimotakanezawa, Haga-machi, Haga-gun, 321-3393, Email: hiroyuki_mae@n.t.rd.honda.co.jp)
2) Keio University (3-14-1, Hiyoshi, Kohoku-ku, Yokohama-shi, 223-8522, Email: oomiya@mech.keio.ac.jp)
3) Tokyo Institute of Technology (2-12-1, O-okayama, Meguro, 152-8552, Email: kkishimo@mep.titech.ac.jp)

The aim of this study is to understand the mechanism governing the transition strain rate of the elastic modulus in semi-crystalline polymer by coarse molecular dynamics (MD). In addition, the effects of the material properties such as molecular weight, crystallinity and lamella thickness on the elastic modulus are studied at various strain rates. The tensile deformation in the crystal direction at the various strain rates is simulated in the lamella MD model. As the results, the strong strain-rate dependency of the elastic modulus becomes prominent when the strain rate is larger than the structural relaxation rate. In addition, the crystallinity is the largest influencing factor on the elastic modulus, compared to the molecular weight and the lamella thickness. The transition strain rate of the elastic modulus gets smaller as the crystallinity increases. This means that the strong strain-rate dependency appears when the strain rate is larger than the relaxation rate of the amorphous phase. This is because the local strain rate of the amorphous phase is larger than that of the macroscopic strain rate.

Key Words: Polymers, Microstructure, Lamella, Elastic Behavior, Strain Rate, Molecular Dynamics

1. Introduction

It is well known that the strong strain-rate dependence, neck propagation, craze creation and growth characterize the large plastic deformation and fracture behavior of the semi-crystalline polymers. As the number of polymer's parts used in the automotive applications gets larger, it is important to consider the mechanical properties of polymers. Polypropylene (PP) is widely used for the automotive components such as instrument panels, bumper skins and door interior panels. The mechanical properties of semi-crystalline polymers have a strong dependency on their morphology and molecular characteristics [1]. In addition to those structural properties, the mechanical properties of polymers depend strongly on the test conditions such as strain rate and temperature. Rolando et al. [2] show that the drastic transition from ductile to brittle for PP films occurred as the strain rate increases. This is because the time for adjusting and absorbing the applied load become shorter. Jang et al. [3] and Olf et al. [4] show that the crazing in the crystalline phase is favored at high deformation rates or low temperature while the shear yielding predominates at low deformation rates or high temperatures. These characteristics are caused by the relaxation of crystalline phase [5]. Alberola et al. [6, 7] obtained that the elastic behavior of quenched and annealed isotactic PP (i-PP) films over a wide strain-rate range from 10^{-3} to 300 s^{-1}. According to Alberora et al. [7], both the crystallinity and the cross-linking of the amorphous phase have the strong effect on the elastic modulus in i-PP films. In addition, it is clearly shown that the strain rate at which the elastic modulus increases for the highly crystallized PP film is slower than that for the low crystallized PP film. Although the effects of the crystallinity and the strain rate on the elastic modulus were clearly shown in the experimental study of Alberora et al. [6, 7], it is still not clear how the crystalline and the amorphous phases behave during the loading, how the trend of those behaviors changes under the different strain rates and how they interact at the interface of those phases. The visco-elastic behavior of polymers is often formulated by spring dashpot models. It is obvious that the resistance to the deformation can change drastically by the relationship between the relaxation rate and the deformation rate. Those deformation processes should be related to the mechanical properties of the semi-crystalline polymers.

Then, the aim of this study is to understand clearly the deformation mechanism which governs the transition strain rate of the elastic modulus in a semi-crystallized PP by coarse-grained molecular dynamics (MD) simulation. The microstructural analyses by coarse-grained MD simulations have been conducted in the craze physics of glassy polymers [8-11]. However, little attention has been paid to the influence

Received (2007. 12. 20), Accepted (2008. 2. 5)

of strain rate and crystallinity on the mechanical properties of semi-crystalline polymers. Hence, it is important to study the effects of the strain rate and the crystallinity on the mechanical behaviors of semi-crystalline polymers from the microscopic point of view. In this paper, the lamella microstructures were modeled with different molecular weights, crystallinities and lamella thicknesses. Then, tensile simulations were conducted by coarse-grained MD. The deformation processes during the tensile deformation and the effects of the molecular weight, crystallinity and lamella thickness on the elastic modulus were discussed.

2. Numerical procedure

The prototypical model in this study is a semi-crystalline thermoplastic polypropylene (PP). The system contains one type of particle, which indicates PP monomers. They are treated as a point mass. Reduced units are used throughout this paper, while all reduced units can be converted to SI units as shown in Table 1. L is the base unit for length, ρ is the reduced density, P is the reduced pressure, $M = \rho L^3$ is the base unit for mass, $\tau = L\sqrt{A_v M / u_o}$ is the base unit for time where A_v is Avogadro's number, $u_0 = P A_v L^3$ is the base unit for energy, and $T=u_0/R$ is the reduced temperature where R is the gas constant. The reduced stress will be later mapped to engineering units. Because of the coarse-grained nature, there is no one-to-one mapping of the model system to the actual system. In this coarse-grained simulation, the goal is to understand the model system self-consistently. In relating the simulation results to the current PP, the emphasis is on the qualitative relationship between deformation rate and relaxation rate.

Table 1 Reduced units converted to SI units

Reduced units	SI units
L	0.65 nm
ρ	$0.85\text{x}10^3$ kg/m^3
P	10 MPa
M	$19.8\text{x}10^{-26}$ kg
τ	5.67 ps
u_0	$1.4\text{x}10^3$ J/mol
T	168.7 K

The dynamics is performed using a Langevin thermostat. Molecular dynamics numerically solves Newton's equations of motion for each particle; particles interact according to a potential energy function U. We employ a set of potentials to model the polymer chains which are standard for dense bead-spring glasses. Beads separated by a distance r interact via a truncated Lennard-Jones potential U_{LJ}.

$$U_{LJ}(r) = 4\varepsilon\left[\left(\frac{\sigma_0}{r}\right)^{12} - \left(\frac{\sigma_0}{r}\right)^{6}\right], \quad r < r_c \tag{1}$$

$$U_{LJ}(r) = 0, \quad r > r_c \tag{2}$$

In this article, σ_0 represents the diameter of LJ sphere and means the strength of the interaction between beads. r_c is the cutoff distance, which means that the beads separated by the distance larger than does not interact. Simulations are conducted for σ_0=1.0L, ε =1.0u_0 and r_c =2.0L. The bonded interaction along the polymer chains is modeled via the finitely extensible non-linear elastic (FENE) potential: [12]

$$U_{bond}(r) = -\frac{1}{2} k R_0^2 \ln\left[1 - \left(\frac{r}{R_0}\right)^2\right] \tag{3}$$

where k is a parameter representing the bond strength, R_0 is a parameter representing the finite extended length. We use standard parameters of $k = 30u_0/L^2$ and $R_0 = 1.5L$ which effectively render impossible the crossing of bonds [12].

The initial lamella structures of chains were generated as shown in Fig. 1. The initial inputs were the length of long period of the semi-crystalline lamella, the length of crystalline phase and the densities of the crystalline and amorphous phase. The details for generating the lamella structure can be found in [13]. For structural relaxation by dynamics simulation, the excluded volume effect is introduced gradually by scaling the forces acting on atoms. The maximum force allowed to act on atoms is given and if the forces become larger than the maximum force, the force is scaled to that value. Then the maximum force for scaling is increased gradually, if the averaged force and the maximum force acting on each atom decrease in the relaxation process, and if the forces acting on all atoms become smaller than the initial maximum force for scaling, the relaxation is completed.

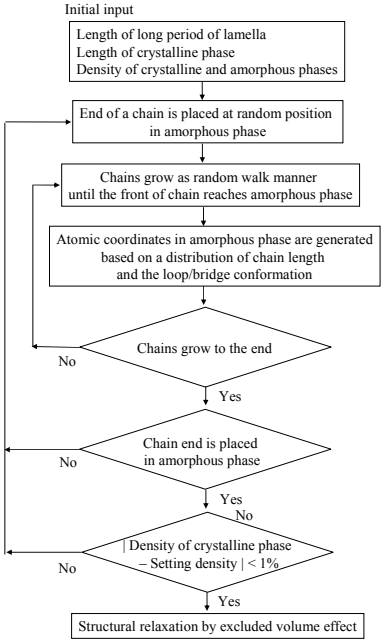

Figure 1 Flow chart of generating lamella structure

For the present simulation, the target polymer is PP. In the previous study [14], the lamella thickness, length of crystalline phase and molecular weight were obtained. Then,

these numbers are used for modeling PP in this study. The unit length: L is set as 0.65 nm because the lattice constant is 0.65 nm in PP. The base unit of mass: M is also determined as 19.8 x 10^{-26} kg because the density of the amorphous phase of PP is 0.85 g/cm^3.[15, 16] The lamella thickness is about 14.8 nm, leading that the simulation domain is a hexahedron (16.1L x 16.1L x 22.75L, where the z-direction is the direction of lamella thickness). The polymer chain is modeled as a straight monomer chain. The polymer chain length of PP was set as 1593 beads because the molecular weight of PP was 190,000 g/mol. The number of polymer chains was decided such that the system density was 1.0, leading to 4 polymer chains of PP in the current model.

The monomers in the simulation domain are evolved through time using the velocity Verlet integration algorithm. The numbers of calculating steps were 50,000 for relaxation with a time step of 0.012τ and 2,000,000 for tensile deformation with a time step of 0.01τ. Periodic boundaries are applied in the x, y and z directions for relaxation and in the x and y directions for tensile deformation because the affine deformation in z direction is applied to the unit cell in the tensile deformation. During the elongation, the stress was calculated based on Virial theorem [13].

Both relaxation and tensile simulations are conducted in the NVT ensemble using a Langevin thermostat [17] with a friction of 0.5 and a set-point temperature of 0.55T. The tensile direction was the crystal direction (z-direction). It is noted that crystalline and amorphous phases are dispersed in semi-crystalline polymers and the tensile direction may be correspond to the mixed direction of the crystal direction and the vertical of the crystal direction. The tensile velocities in the z-direction were $0.0001L/\tau$, $0.001L/\tau$, $0.01L/\tau$, $0.1L/\tau$ and $1.0L/\tau$ for the crystal direction. The tensile velocity of $1.0L/\tau$ corresponded to the strain rate of 0.044 τ^{-1}. Because of the coarse-grained nature, the strain rate is much faster than the quasi-static deformation. However, it is shown that the structure of the current model is relaxed enough during the slowest deformation in the snapshots of the deformation of lamella structure. Thus, it is assumed that the current model can cover the deformation range of ductile-brittle transition qualitatively. Figure 2 shows the initial model with crystalline phase and amorphous phase after relaxation.

In this study, the elastic modulus was evaluated. In the crystal direction elongation, it is expected that the effect of the crystallinity on the elastic modulus is the strongest, leading to the clear understanding of the effect of the crystallinity. The qualitative analyses were conducted focusing on the transition strain rate of the apparent elastic modulus with the strain rates and the crystallinities. The studied crystallinities were 0.57, 0.71 and 0.86. In addition, the effects of molecular weight and lamella thickness on the apparent elastic modulus were studied. The molecular weights were 95,000, 190,000 and 380,000 g/mol. The lamella thicknesses were 7.4, 14.8 and 29.6 nm. In changing the molecular weight, the number of polymer chains was changed such that the system density was 1.0, leading to 8 polymer chains for the molecular weight of 95,000 g/mol, 2 polymer chains for the molecular weight of 380,000 g/mol. In changing the crystallinity and lamella thickness, the number of polymer chains was kept same as the base model.

The simulation code used in this study was the standard coarse-grained molecular dynamics model with public domain meso-scale simulation code COGNAC [13] inside an integrated simulation system for soft materials OCTA [18].

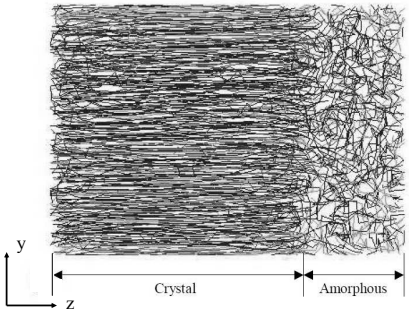

Figure 2 Numerical model of lamella structure

3. Result of tensile simulation

Figure 3 shows the simulated stress-strain curves at the various tensile strain rates when the lamella model of the molecular weight of 190,000 at the crystallinity of 0.71 is elongated to the crystal direction. It is clearly shown that the stress increases drastically at the strain rates above 4.4 x 10^{-4} τ^{-1}. As the strain rates increase, the strain at which the stress increases drastically gets smaller. It is considered that the limited elongation length of spring model caused the drastic increase of the stress value, which means that the spring models finished elongating more rapidly at the high strain rates than that at the low deformation rates. Figure 4 shows the relationship between the elastic modulus and the deformation rates. The elastic modulus increases as the deformation rate increases. The clear transition is observed at the strain rate of around 4.4 x 10^{-4} τ^{-1}. At the strain rate of 4.4 x 10^{-2} τ^{-1}, the elastic modulus increases about 5 times as large as that at the strain rate of 4.4 x 10^{-3} τ^{-1}. Figure 5 shows the simulated deformation snapshots at the strain rates of 4.4 x 10^{-5} τ^{-1} and 4.4 x 10^{-3} τ^{-1}. In Fig. 4(a), the structural relaxation of the lamella phase can be observed during the elongation process and the lamella phase transforms into the amorphous phase. On the contrary, at the strain rates of 4.4 x 10^{-3} τ^{-1}, the lamella phase keeps its structure and is elongated to the loading direction. The

structural relaxation of the lamella phase can not be observed. Further, the amorphous phase is largely elongated and the fibril structures are formed at the interface between the lamella and amorphous phases as shown in Fig. 5(b). It is considered that the microstructural deformation mechanism changes between the strain rate of 4.4 x 10^{-4} τ^{-1} and 4.4 x 10^{-3} τ^{-1}, leading to the deformation-rate dependency of stress-strain relationship.

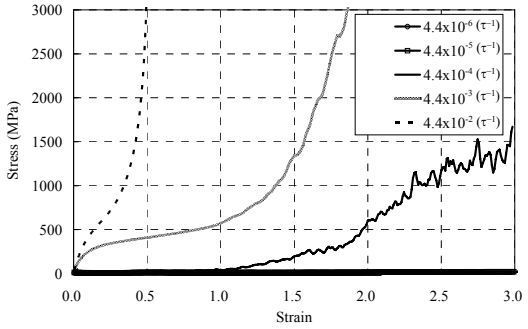

Figure 3 Stress-strain curves at various strain rates

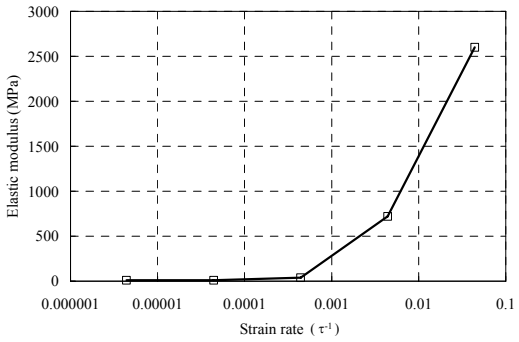

Figure 4 Relationship between the elastic modulus and the strain rates

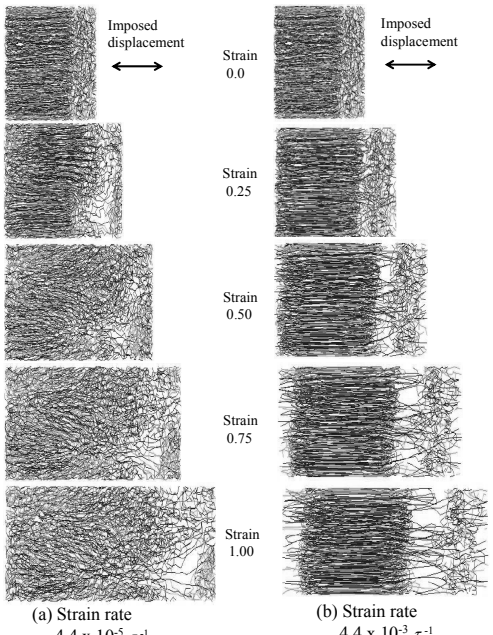

Figure 5 Snapshot of deformation of lamella model

4. Effects of molecular weight, crystallinity and lamella thickness on the elastic modulus

By using the same numerical model, the effects of molecular weight, crystallinity and lamella thickness on the elastic modulus were studied. The elastic modulus is plotted against the deformation rates in the molecular weights in Fig. 6. As shown clearly, the dependency of the molecular weight was not observed in the elastic modulus at the strain rate of 4.4 x 10^{-3} τ^{-1}. At the strain rates ranging from 4.4 x 10^{-5} τ^{-1}, to 4.4 x 10^{-2} τ^{-1}, the elastic modulus is independent of molecular weights. Figure 7 shows the effects of the crystallinities and the strain rates on the elastic modulus. The elastic modulus had strong dependency on the crystallinity. The elastic modulus increases as the crystallinity gets larger. This result coincides with the results where the tensile elastic modulus increases with the larger crystallinity [7]. In addition, the interesting result is that the strain rate at which the elastic modulus increases gets smaller as the crystallinity increases. The dependency of the elastic modulus on the crystallinity also agrees with the experimental results [7]. It is considered that the relaxation rates in the crystal phase as well as the amorphous phase might cause the changes of the transition strain rates. Figure 8 shows the effect of lamella thickness and strain rate on the elastic modulus. The elastic modulus at the strain rate of 4.4 x 10^{-3} τ^{-1} is almost same as shown in Fig. 8. The elastic modulus does not have the lamella-thickness dependency at the strain rates studied here.

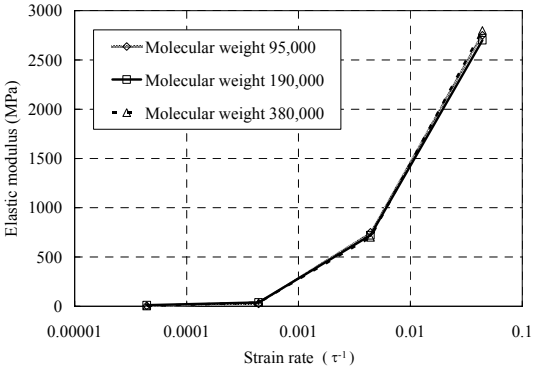

Figure 6 Effects of the molecular weights and the deformation rates on the elastic modulus

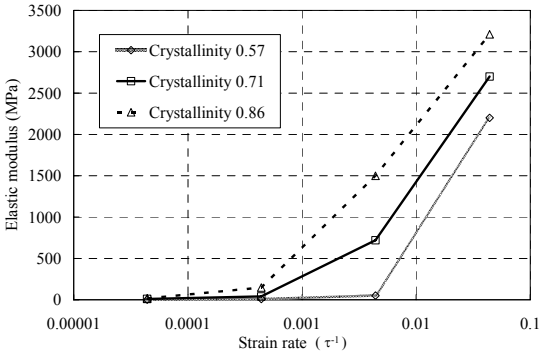

Figure 7 Effects of the crystallinities and the deformation rates on the elastic modulus

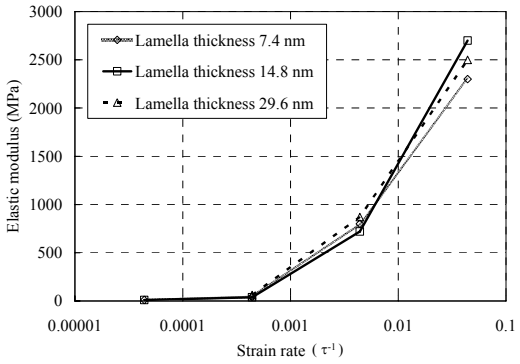

Figure 8 Effects of the lamella thicknesses and the deformation rates on the elastic modulus

5. Discussion

The most interesting result in this study was the effect of strain rate and the crystallinity on the elastic modulus as shown in Fig. 7. Let us consider this result from the point of view of the lamella structural relaxation rate. In general, it is well known that there are various relaxation processes of polymers [19]. For examples, the short-time period of relaxation processes are the micro blown movement of C-C chain and the movement of $-CH_3$ while the long-time period of relaxation process is the entanglement release of the whole molecular chains in the macroscopic scale. If the deformation rate is slower than the relaxation rate in the lamella structure, the structural relaxation of the lamella phase is induced by the applied deformation as shown in Fig. 5(a). Then, the lamella structure changes to the amorphous-like structure during deformation process. On the contrary, when the deformation rate is faster than the relaxation rate, the structural relaxation of the lamella phase does not occur as shown in Fig. 5(b). Thus, it is suggested that the transition deformation rate of the elastic modulus is strongly related to the relaxation rate.

Another issue in Fig. 7 is why the transition strain rate gets slower as the crystallinity increases. It is well known that the relaxation rate is faster in the crystal phase than in the amorphous phase [19]. Here, let us consider the simulated lamella model as two Maxwell spring dashpot models where the first one corresponds to the crystal phase and the second one is the amorphous phase as shown in Fig. 9(a). Let us assume that the dashpot should work only when the strain rate is faster than the relaxation rate in each phase, for simply explaining the mechanism. Figure 9(b) shows the case when the strain rate is slower than the relaxation rates of both crystal and amorphous phases. It is considered that the effect of the dashpots in the crystal and amorphous phases is quite small, since entanglements and frictions between molecular chains are small due to the relaxation. This leads to small resistance against the applied deformation. Fig. 9(c) shows the case when the strain rate is between the relaxation rates of the crystal and amorphous phases. In this particular case, the amorphous phase can not relax while the crystal phase relaxes. In the amorphous phase, it is considered that the effect of the dashpot appears because of the entanglements and frictions of the molecular chains, leading to the strain-rate dependency of the elastic modulus. Then the dashpot of the amorphous phase works against the applied load. As a result, both the reactive forces of the spring and the dashpot in the amorphous phase lead to the strain-rate dependency of the elastic modulus. Further, in the case when the strain rate is faster than both relaxation rates of the crystal and amorphous phases, the dashpot of the crystal phase also works. In addition, the strong reactive force of the spring in the crystal phase is added, which leads the strain-rate dependent elastic modulus caused by both the spring and the dashpot of the crystal phase.

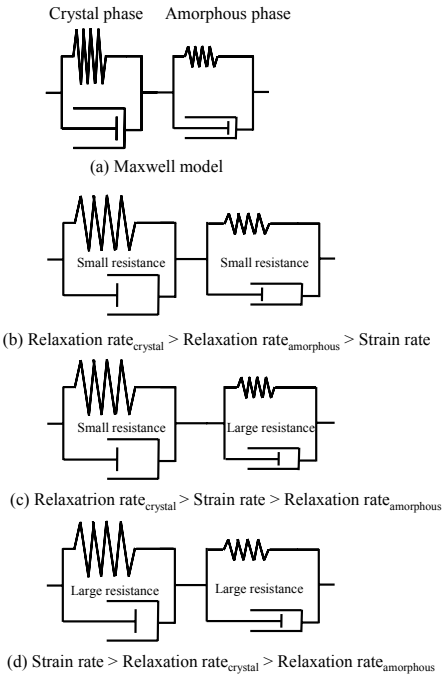

Figure 9 Maxwell spring dashpot models

Based on the above discussion, it is suggested that the strain-rate dependency of the elastic modulus should appear, once the applied strain rate is faster than the relaxation rate of the amorphous phase as shown in Figs. 9(c) and (d). In addition, the deformation occurred preferentially in the amorphous phase as shown in Fig. 5(b). Then, it is considered that the strain-rate dependency of the elastic modulus appears mainly when the local strain rate of the amorphous phase is faster than the relaxation rate of the amorphous phase. Thus, when the crystallinity is larger leading to the smaller amorphous thickness, the local strain rate in the amorphous phase gets faster than the whole strain rate of the lamella structure. This is the reason why the elastic modulus starts increasing at the slower strain rate when the crystallinity is larger. In addition, it is suggested that the dashpot of the crystal phase is activated between the strain rates of 4.4×10^{-3}

τ^{-1} and 4.4 x 10^{-2} τ^{-1} in Fig.4 because it is considered that the increase of slope of the elastic modulus is caused by the dashpot of the crystal phase as shown in Fig. 9(d). Figure 10 shows the plot modified by the local strain rate of the amorphous phase based on Fig. 7. As shown clearly, the dependency of the crystallinity disappears by considering the local strain rate of the amorphous phase. In addition, the effect of the crystallinity on the elastic modulus in the perpendicular direction of the crystal direction was not observed because it is expected that the local deformation rate was almost same as the macroscopic strain rate. These results coincide with the above suggestion.

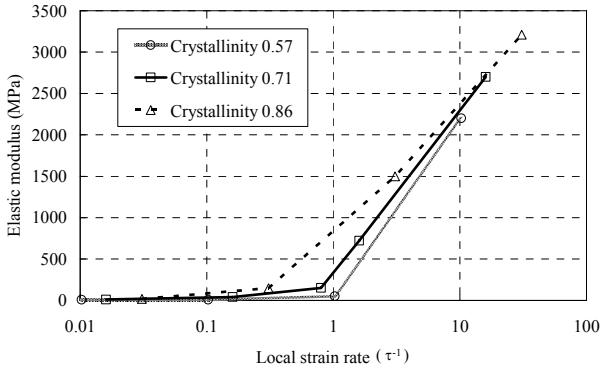

Figure 10 Elastic modulus plotted against local strain rates of the amorphous phase

6. Conclusion

The relationship between the strain rate and the structural relaxation rate for semi-crystalline polymer was studied by coarse-grained molecular dynamics simulation. In addition, the effects of the material properties such as molecular weight, crystallinity and lamella thickness on the elastic modulus in the crystal direction were studied at various deformation rates. The followings are the conclusions of this study.

(1) The strong strain-rate dependency of elastic modulus is caused by the relationship between the strain rate and the structural relaxation rate and it occurs when the strain rate is faster than the relaxation rate of the amorphous phase.

(2) The crystallinity is the most influence factor on the elastic modulus compared to the molecular weight and the lamella thickness.

(3) The transition deformation rate of the elastic modulus gets smaller as the crystallinity increases. It is because that the local strain rate in the amorphous phase gets faster than the whole strain rate, when the crystallinity is larger leading to the smaller amorphous thickness.

For the applications in automobile, especially crash applications, the strain rate dependency is the most important characteristic in polymer materials. This study shows the local strain rate in the amorphous phase of the lamella model is larger than that of the macroscopic one. Therefore, more detailed studies are encouraged. Especially, the experimental study about the relations between the macroscopic elastic modulus and the microscopic elastic modulus in lamella scale is left as future works.

References

[1] J. N. Chu and J. M. Schultz, “The influence of microstructure on the failure behavior of PEEK”, J. Mater. Sci., 24, 4538 (1989).

[2] R. J. Rolando, D. L. Lrueger and H. W. Morri, “The influence of morphology on the tensile properties of polypropylene”, Polym. Mater. Sci. Eng., 52, 76 (1985).

[3] B. Z. Jang, D. R. Uhlmann and J. B. Vander Sande, “Crazing in polypropylene”, Polym. Eng. Sci., 25, 98 (1985).

[4] H. G. Olf, A. Peterlin and W.L. Peticolas, “Laser-raman study of the longitudinal acoustic mode in polypropylene”, J. Polym. Sci., 12, 2209 (1974).

[5] T. Ree and H. Eyring, “Theory of non-Newtonian flow. I. Solid plastic system”, J. Appl. Phys., 26, 793 (1955).

[6] N. Alberola, M. Fugier, D. Petit and B. Fillon, Microstructure of quenched and annealed films of polypropylene”, J. Mater. Sci., 30, 1187 (1995).

[7] N. Alberola, M. Fugier, D. Petit and B. Fillon, “Tensile mechanical behavior of quenched and annealed isotactic PP films”, J. Mater. Sci., 30, 860 (1995).

[8] A. R. C. Baljon and M. O. Robbins, “Energy dissipation during rupture of adhesive bonds”, Science, 271, 482 (1996).

[9] A. R. C. Baljon and M. O. Robbins, “Simulations of crazing in polymer glasses: Effect of chain length and surface tension”, Macromol., 271, 482 (1996).

[10] J. Rottler, S. Barsky and M.O. Robbins, “Cracks and crazes: On calculating the macroscopic fracture energy of glassy polymers from molecular simulations”, Phys. Rev. Lett., 89, 148304 (2002).

[11] J. Rottler and M.O. Robbins, “Growth, microstructure, and failure of crazes in glassy polymers”, Phys. Rev. E., 68, 011801 (2003).

[12] K. Kremer and G. S. Grest, “Dynamics of entangled linear polymer melts: A molecular dynamics simulation”, J. Chem. Phys., 92, 8, 5057 (1990).

[13] COGNAC User’s Manual Version 4.2.4, 2005.

[14] H. Mae, M. Omiya and K. Kishimoto, “Microstructural observation and simulation of micro damage evolution of polypropylene blended with ethylene-propylene-rubber and talc”, submitted for publication (2008).

[15] D. N. Theoforou and U. W. Suter, “Atomistic modeling of mechanical properties of polymeric glasses”, Macromolecules, 19, 139 (1986).

[16] Example Manual in AMUSE 2.2.3.3, 2005

[17] Frenkel, D., Smit, B., Understanding Molecular Simulation, 2nd ed., Academic Press, San Diego (2001).

[18] M. Doi, “OCTA (Open Computational Tool for Advanced material technology”, Macromol. Sym., 195, 101 (2003).

[19] G. R. Strobl, The Physics of Polymers, Springer (1997).